Approximate Model for Diffusion and Reaction in a Porous Catalyst with Mass-Transfer Resistances

Mirosław K. Szukiewicz
Dept. of Chemical Engineering and Process Control, Rzeszów University of Technology, al. Powstańców Warszawy 6, 35-959 Rzeszów, Poland

Mathematical modeling of diffusion and reaction processes is a very strong tool for design and research. Unfortunately, for the devices most often applied in industry (for example, fixed-bed reactors) models are sophisticated with a high degree of complexity. Mathematically, the models are PDE systems (boundary-value problems), which are difficult and/or take a long time to solve. A commonly applied effectiveness factor concept reduces the equation set of the model and facilitates finding a solution. Applying the approximate model concept [namely, replacing the mass-balance PDE for a pellet by a proper ODE; this concept is fully described in the article by Szukiewicz (2000), and in the references presented there] also yields a substantial simplification for analysis and calculations. It does not require any iterative and trial-and-error computations.

The approximate models reported so far in the literature took into account the spherical particles with no mass-transfer limitations. In the present work approximate linear-driving force models of a catalyst particle for planar, cylindrical, and spherical geometry of the pellet concerning external mass-transfer resistance are developed. The mathematical part of this article is based on a complex analysis (Laplace-Carson transform) and is quite difficult, but the formulas obtained are both easy to understand (each term of the formulas has physical meaning) and to solve (mathematically, the approximate formula is a linear ODE). Accuracy of the approximation is very high over the entire range of Φ, regardless of the external mass-transfer resistances and geometry of the pellet.

Theory

The method of derivation of approximate models applied in this article was elaborated in detail in the article by Szukiewicz (2000). Here, only the basic transformations of equations will be presented. All equations are presented in dimensionless form. Concentrations are related to maximum component concentration, while distance is related to the characteristic dimension of a pellet (a half of the thickness for a slab and a radius for cylinder and sphere).

Assuming a linear kinetic rate, transient diffusion and the reaction process in a porous pellet can be described as

$$\frac{\partial c}{\partial \tau} = \frac{1}{x^a}\frac{\partial}{\partial x}\left(x^a \frac{\partial c}{\partial x}\right) - \Phi^2 c, \tag{1}$$

where $a = 0$, 1, 2 for the planar, cylindrical, and spherical geometry of the pellet, respectively.

$$\text{IC:} \quad c(0, x) = c_{\text{in}} \tag{2}$$

$$\text{BC:} \quad \left.\frac{\partial c}{\partial x}\right|_{x=0} = 0 \tag{3}$$

$$\left.\frac{\partial c}{\partial x}\right|_{x=1} = Bi_m[c_0(\tau) - c(\tau, 1)]. \tag{4}$$

The Thiele modulus and Biot number are defined as follows:

$$\Phi = L\sqrt{k_1/D_{ef,A}}; \quad Bi_m = k_{g,A}L/D_{eff,A}.$$

In the text below, capital letters are used to describe the complex functions corresponding to the real functions in the Laplace-Carson transform. Moreover, to simplify the notation the parameter $\sqrt{\Phi^2 + p}$ will be denoted as μ.

Applying the Laplace-Carson transform, the complex solution of the model for a sphere ($a = 2$) can be described as

$$C = \frac{1}{x}\frac{Bi_m\left(C_0 - \dfrac{pc_{\text{in}}}{\mu^2}\right)\sinh(\mu x)}{\mu\cosh\mu - \sinh\mu + Bi_m\sinh\mu} + \frac{pc_{\text{in}}}{\mu^2}. \tag{5}$$

The average concentration in the pellet is given by

$$C_{\text{av}} = (a+1)\int_0^1 Cx^a\,dx, \tag{6}$$

where $a = 0$, 1, 2 for the planar, cylindrical, and spherical geometry of the pellet, respectively.

Substituting for C and integrating the results gives

$$C_{\text{av}} = \frac{3Bi_m\left(C_0 - \dfrac{pc_{\text{in}}}{\mu^2}\right)(\mu\cosh\mu - \sinh\mu)}{\mu^2(\mu\cosh\mu - \sinh\mu + Bi_m\sinh\mu)} + \frac{pc_{\text{in}}}{\mu^2}. \tag{7}$$

The latest equation can be rearranged to

$$pC_{av} - pc_{in} = \frac{3Bi_m \mu^2(\mu\cosh\mu - \sinh\mu)}{\mu^2(\mu\cosh\mu - \sinh\mu + Bi_m\sinh\mu) - 3Bi_m(\mu\cosh\mu - \sinh\mu)} \times (C_0 - C_{av}) - \Phi^2 C_{av}. \quad (8)$$

This equation is the Laplace-Carson transform of the following LDF formula. For a constant value of the first term of the righthand side (before parenthesis) of Eq. 8, the equation can be easily converted to the real domain form. For τ approaching infinity (it corresponds to p approaching 0), the value of the term just mentioned is constant and equal to

$$\lim_{p\to 0} \frac{3Bi_m \mu^2(\mu\cosh\mu - \sinh\mu)}{\mu^2(\mu\cosh\mu - \sinh\mu + Bi_m\sinh\mu) - 3Bi_m(\mu\cosh\mu - \sinh\mu)} = \frac{3Bi_m\Phi^2(\Phi\cosh\Phi - \sinh\Phi)}{\Phi^2(\Phi\cosh\Phi - \sinh\Phi + Bi_m\sinh\Phi) - 3Bi_m(\Phi\cosh\Phi - \sinh\Phi)} = \frac{3}{\frac{1}{Bi_m} + \frac{\Phi^2\sinh\Phi - 3(\Phi\cosh\Phi - \sinh\Phi)}{\Phi^2(\Phi\cosh\Phi - \sinh\Phi)}}. \quad (9)$$

Hence, Eq. 8 can be written as

$$pC_{av} - pc_{in} = \frac{3}{\frac{1}{Bi_m} + \frac{\Phi^2\sinh\Phi - 3(\Phi\cosh\Phi - \sinh\Phi)}{\Phi^2(\Phi\cosh\Phi - \sinh\Phi)}} \times (C_0 - C_{av}) - \Phi^2 C_{av}. \quad (10)$$

The inverse transform of this equation gives the following approximate formula

$$\frac{\partial c_{av}}{\partial\tau} = \frac{3}{\frac{1}{Bi_m} + \frac{\Phi^2\sinh\Phi - 3(\Phi\cosh\Phi - \sinh\Phi)}{\Phi^2(\Phi\cosh\Phi - \sinh\Phi)}} \times (c_0 - c_{av}) - \Phi^2 c_{av} \quad (11)$$

$$\text{IC:} \qquad c_{av}(0) = c_{in}. \quad (12)$$

The last term in the denominator is the reciprocal of the quantity Ψ defined in the earlier work as an approximate model of the spherical particle with no mass-transfer limitations.

The linear driving-force formulas for other pellet geometry have been derived analogously. Like the former model, the approximate model of the pellet can be written in the following compact form

$$\frac{\partial c_{av}}{\partial\tau} = \frac{a+1}{\frac{1}{Bi_m} + \frac{1}{\Psi_a}}(c_0 - c_{av}) - \Phi^2 c_{av} \quad (13)$$

$$\text{IC:} \qquad c_{av}(0) = c_{in}, \quad (14)$$

where $a = 0$, 1, 2 for the planar, cylindrical, and spherical geometry of the pellet, respectively, and

$$\Psi_0 = \frac{\Phi^2\sinh\Phi}{\Phi\cosh\Phi - \sinh\Phi} \quad (15)$$

$$\Psi_1 = \frac{\Phi^2 I_1(\Phi)}{\Phi I_0(\Phi) - 2I_1(\Phi)} \quad (16)$$

$$\Psi_2 = \frac{\Phi^2(\Phi\cosh\Phi - \sinh\Phi)}{\Phi^2\sinh\Phi - 3(\Phi\cosh\Phi - \sinh\Phi)}, \quad (17)$$

where I_0 and I_1 are the modified Bessel functions.

On the basis of the preceding equations the following relationship between the parameter Ψ and the well-known local effectiveness factor can be derived:

$$\Psi_a = \frac{\Phi^2}{(a+1)\left(\frac{1}{\eta_a} - 1\right)}, \quad (18)$$

where $a = 0$, 1, 2 for the planar, cylindrical, and spherical geometry of the pellet, respectively, and η_a is the local effectiveness factor for the slab, cylinder, and sphere, respectively.

One advantage of the model is that it clearly characterizes the influence of the external and internal mass-transfer resistances on the overall mass-transfer process between the pellet and its surroundings. If the external mass-transfer resistance is negligible (Bi_m approaches infinity) for the spherical particle, the model reduces to the form presented and elaborated in the previous article.

Results and Discussion

Analyzing both the exact model—Eqs. 1–4—and the approximate one—Eqs. 13–14—it is easy to perceive their similarities. Both models include accumulation, mass-transfer rate, and mass-generation rate. Furthermore, accumulation and kinetic rate have the same form, but the first model is a distributed-parameter model with a position-dependent concentration, while the second one is a lumped-parameter model with an average concentration. The difference occurs in the term describing the mass-transfer process between the pellet and its surroundings. In the exact model, intraparticle mass transfer is described by the first term on the righthand side of Eq. 1, while external mass transfer is described by one of the boundary conditions. In the approximate model, both the external and internal mass-transfer resistances affect a

value of one parameter only, namely

$$\alpha = \frac{a+1}{Bi_m^{-1} + \Psi_a^{-1}}. \tag{19}$$

The influence of both resistances on this parameter is obvious. Figure 1 shows the influence of the Biot number and Thiele modulus on the value of the parameter just defined. Regardless of the pellet geometry, the value of α increases with the Thiele modulus as the external mass-transfer resistances grow less. It is a reflection of the rapidity in the mass transfer rate resulting from the chemical reaction. Also note that the smaller the value of Bi_m, the smaller the differences in value of α, especially for larger values of Φ.

Tests of the compatibility of the models were performed in two steps for $\Phi \in [0 \cdots 20]$ and $Bi_m \in [10, 100, 1{,}000, \infty]$:

1. For time-independent bulk concentration $c_0 = 1$;
2. For time-dependent bulk concentration $c_0 = 0.5 + A\sin(\omega\tau)$; $A = [0.5, 0.1, 0.05]$, $\omega = [1, 5, 20]$. In addition, it is assumed that $c_{\text{in}} = 0$.

An analytical solution of the exact model—Eqs. 1–4—for a sphere and time-independent bulk concentration $c_0 = 1$ (Goto et al., 1990; this article also contains a solution for the slab) is given by

$$c_{\text{exact}} = \frac{(Bi_m/x)\sinh(\Phi x)}{\Phi\cosh\Phi + (Bi_m - 1)\sinh\Phi} + \frac{2Bi_m}{\Phi x} \times \sum_{n=1}^{\infty} \frac{\sqrt{\lambda_n}\sin\left(\Phi x\sqrt{\lambda_n}\right)}{(\lambda_n + 1)\left[Bi_m\cos\left(\Phi\sqrt{\lambda_n}\right) - \Phi\sqrt{\lambda_n}\sin\left(\Phi\sqrt{\lambda_n}\right)\right]} e^{-(\lambda_n+1)\tau}, \tag{20}$$

and, the volume-averaged concentration (according to Eq. 6) is given by

$$c_{\text{av,exact}} = \frac{3Bi_m(\Phi\cosh\Phi - \sinh\Phi)}{\Phi^2\left[\Phi\cosh\Phi + (Bi_m - 1)\sinh\Phi\right]} + \frac{6Bi_m}{\Phi^3} \times \sum_{n=1}^{\infty} \frac{-\Phi\sqrt{\lambda_n}\cos\left(\Phi\sqrt{\lambda_n}\right) + \sin\left(\Phi\sqrt{\lambda_n}\right)}{(\lambda_n + 1)\sqrt{\lambda_n}\left[Bi_m\cos\left(\Phi\sqrt{\lambda_n}\right) - \Phi\sqrt{\lambda_n}\sin\left(\Phi\sqrt{\lambda_n}\right)\right]} \times e^{-(\lambda_n+1)\tau}. \tag{21}$$

In the preceding equations λ_n can be determined from the transcendental equation:

$$\Phi\sqrt{\lambda_n}\cos\left(\Phi\sqrt{\lambda_n}\right) + (Bi_m - 1)\sin\left(\Phi\sqrt{\lambda_n}\right) = 0. \tag{22}$$

While the solution of the approximate model can be expressed much more easily

$$c_{\text{av,app}} = \frac{\dfrac{3}{\dfrac{1}{Bi_m^{-1} + \Psi_2^{-1}}}}{\dfrac{3}{Bi_m^{-1} + \Psi_2^{-1}} + \Phi^2}\left[1 - e^{-[(3)/(Bi_m^{-1} + \Psi_2^{-1}) + \Phi^2]}\right]. \tag{23}$$

The preceding equations illustrate the benefit of the LDF approach: simple, algebraic equation (Eq. 23) instead of the series (Eq. 21) with the transcendental equation (Eq. 22). The accuracy of the approximate model is very good for a sufficiently long time (it is showed below, e.g., Table 1). Results obtained both for the planar, cylindrical, and spherical geometries confirmed, in principle, all the conclusions that were drawn in the previous article for neglecting external mass resistances. It is the reason the analogous conclusions will be presented here without discussion. The proposed LDF formulas approximate the exact solution very well over the entire range of Φ regardless of external mass resistances. A maximum error does not exceed 1% for the largest Φ at steady state. The only difference with respect to the case of no mass-transfer limitations is that the inequality determining the valid range of the approximate model has to be slightly modified. As presented below, the inequality shows the influence of the Biot number on the accuracy of the calculations.

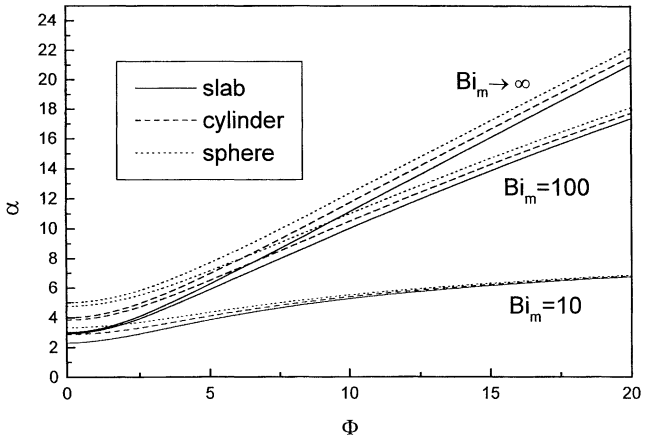

Figure 1. Parameter α vs. Thiele modulus for slab, cylinder, and sphere for selected values of Biot number.

$$\tau \geq \frac{5}{\dfrac{a+1}{Bi_m^{-1} + \Psi_a^{-1}} + \Phi^2}. \tag{24}$$

Of course, both terms in the denominator (α and Φ^2) affect the time determined by Eq. 24, but an analysis of Figure 1 leads to the conclusion that the term Φ^2 dominates for larger Φ. Next, the smaller the value of Bi_m, the greater its influence on parameter α. Thus, for an arbitrary value of Bi_m and for Φ as it approaches 0 (case of no reaction), a larger influence of the Biot number on the accuracy of calculations is expected, and this influence vanishes if Φ rises. Some results of the calculations that illustrate these observations are shown in Table 1. Regardless of Φ, the compatibility of the calculations increases as time passes. For $\Phi = 0$ and large mass-transfer resistance, the time after which full compatibility of results is observed is longer than when there is no resistance. This effect practically vanishes for intermediate mass-transfer resistance. For $\Phi = 1$, the difference mentioned earlier is barely visible, and for larger Φ it is not seen. It is worth noting that for an arbitrary value of Φ, the smaller the

average error, the smaller the value of Bi_m. Thus the greater the external mass-transfer resistance, the closer the linear driving-force formula approximates the exact solution.

And finally, a brief comparison of the two simplification concepts of a heterogeneous reactor model is presented. Applying the effectiveness factor concept nearly reduces the heterogeneous reactor model to a homogeneous one. These models differ by only one parameter (namely by the effectiveness factor). It is very convenient, since the analysis is practically the same for both models, and moreover, the value of the effectiveness factor directly describes the solid-state influence on the reaction rate. The concept of an approximate model reduces the distributed-parameter model of the pellet to a lumped-parameter model. It is also a substantial simplification. The heterogeneous reactor model still contains separate equations for mass balance in a fluid and in a pellet, but finding a solution is much simpler. In contrast to the effectiveness-factor concept, the approximate model enables us to investigate the dynamic behavior of the pellet. It can be crucial for models applied in the process control field, for example. Especially, approximate models make it possible to take the external mass-transfer resistances into account naturally. Each of the concepts has both advantages and drawbacks and, in my opinion, the choice of whether to apply any of the simplifying concepts or even a nonsimplified model is up to a researcher.

Conclusions

The proposed approximate model, Eqs. 13–14, extends the validity of the formula proposed in the article by Szukiewicz (2000) for any type of pellet geometry, and it especially takes the case of external mass-transfer limitations into account. The conclusions presented in the cited article are valid for this model, with the small difference regarding the time-validity range of the approximate model. This difference is of importance only for large external mass-transfer resistances and small values of the Thiele modulus, which were discussed earlier in this article.

The accuracy of the approximation is very high over the entire range of Φ, regardless of external mass-transfer resistances and the geometry of the pellet. The maximum error does not exceed 1% for the largest Φ at steady state. The accuracy increases as time passes, and the simple relation (Eq. 24) that defines the model's validity range is presented. In agreement with the relation proposed, the LDF model can be used for higher Thiele modulus values for almost the entire time scale.

Table 1 Average Concentration in the Slab ($a = 1$) vs. Time for Selected Values of Thiele Modulus and Biot Number

τ	$c_{\mathrm{av,exact}}$	$c_{\mathrm{av,app}}$	δ (%)	$c_{\mathrm{av,exact}}$	$c_{\mathrm{av,app}}$	δ (%)	$c_{\mathrm{av,exact}}$	$c_{\mathrm{av,app}}$	δ (%)
	$\Phi = 0.0,\ Bi_{\mathrm{m}} = \infty$			$\Phi = 0.0,\ Bi_m = 100$			$\Phi = 0.0,\ Bi_m = 10$		
0.1	0.421	0.333	20.6	0.412	0.327	20.6	0.346	0.285	17.6
0.3	0.652	0.634	2.7	0.643	0.624	2.9	0.573	0.550	4.1
0.5	0.788	0.799	1.5	0.780	0.790	1.3	0.716	0.716	0.1
0.7	0.870	0.890	2.2	0.865	0.883	2.1	0.812	0.821	1.2
0.9	0.921	0.940	2.0	0.916	0.935	2.0	0.875	0.887	1.4
1.1	0.952	0.967	1.6	0.949	0.963	1.6	0.917	0.929	1.3
1.3	0.970	0.982	1.2	0.968	0.980	1.2	0.945	0.955	1.1
1.5	0.982	0.990	0.8	0.980	0.989	0.8	0.963	0.972	0.9
1.7	0.989	0.995	0.6	0.988	0.994	0.6	0.976	0.982	0.7
1.9	0.993	0.997	0.4	0.993	0.996	0.4	0.984	0.989	0.5
2.1	0.996	0.998	0.2	0.995	0.998	0.3	0.989	0.993	0.4
2.3	0.997	0.999	0.2	0.997	0.999	0.2	0.993	0.996	0.3
2.5	0.998	1.000	0.1	0.998	0.999	0.1	0.995	0.997	0.2
2.7	0.999	1.000	0.1	0.999	1.000	0.1	0.997	0.998	0.1
2.9	1.000	1.000	0.0	1.000	1.000	0.0	0.999	0.999	0.0
	$\Phi = 1.0,\ Bi_m = \infty$			$\Phi = 1.0,\ Bi_m = 100$			$\Phi = 1.0,\ Bi_m = 10$		
0.1	0.403	0.327	19.0	0.395	0.320	18.8	0.329	0.276	16.1
0.3	0.586	0.574	2.2	0.577	0.564	2.4	0.507	0.490	3.4
0.5	0.674	0.680	0.9	0.666	0.671	0.8	0.599	0.598	0.1
0.7	0.718	0.726	1.2	0.710	0.719	1.1	0.648	0.652	0.6
0.9	0.740	0.746	0.9	0.733	0.739	0.9	0.675	0.680	0.6
1.1	0.751	0.755	0.6	0.744	0.749	0.6	0.690	0.694	0.5
1.3	0.756	0.759	0.3	0.750	0.753	0.4	0.698	0.701	0.4
1.5	0.759	0.760	0.2	0.753	0.754	0.2	0.702	0.704	0.2
1.7	0.760	0.761	0.1	0.754	0.755	0.1	0.705	0.706	0.1
1.9	0.761	0.761	0.1	0.755	0.756	0.1	0.706	0.707	0.1
	$\Phi = 3.0,\ Bi_m = \infty$			$\Phi = 3.0,\ Bi_m = 100$			$\Phi = 3.0,\ Bi_m = 10$		
0.1	0.300	0.271	9.4	0.290	0.263	9.3	0.228	0.209	8.2
0.3	0.329	0.328	0.3	0.319	0.318	0.4	0.253	0.251	0.6
0.5	0.331	0.331	0.0	0.322	0.322	0.0	0.255	0.255	0.0
	$\Phi = 5.0,\ Bi_m = \infty$			$\Phi = 5.0,\ Bi_m = 100$			$\Phi = 5.0,\ Bi_m = 10$		
0.1	0.200	0.196	2.3	0.191	0.186	2.3	0.134	0.131	2.2
0.3	0.200	0.200	0.0	0.190	0.190	0.0	0.133	0.133	0.0

Note: relative error: $\delta = 100\ (c_{av,ex} - c_{av,app})/c_{av,ex}$.

Notation

A = coefficient
c = dimensionless concentration of component A
c_{av}, c_{in}, c_0 = dimensionless concentration of component A: average, initial, and bulk, respectively
c_{app}, c_{exact} = general notation for results obtained from approximate and exact model, respectively
$D_{eff,A}$ = effective diffusity of component A
k_1 = reaction rate constant
$k_{g,A}$ = mass-transfer coefficient
L = characteristic dimension of a pellet
p = complex variable

Greek letters

δ = relative error
$\tau = tD_{ef,A}/L^2$ = dimensionless time
ω = coefficient
Ψ_0, Ψ_1, Ψ_2 = parameters defined by Eqs. 15, 16, and 17, respectively

Literature Cited

Goto, M., J. M. Smith, and B. J. McCoy, "Parabolic Profile Approximation (Linear Driving-Force Model) for Chemical Reactions," *Chem. Eng. Sci.*, **45**, 443 (1990).
Szukiewicz, M. K., "New Approximate Model for Diffusion and Reaction in a Porous Catalyst," *AIChE J.*, **46**, 661 (2000).

Manuscript received May 22, 2000, and revision received Sept. 21, 2000.